

Ti-base alloy coking behavior during steam cracking of ethane

*Stamatis A. Sarris, Marie-Françoise Reyniers, Kevin M. Van Geem, Guy B. Marin
Ghent University, Laboratory for Chemical Technology, Technologiepark 914, 9052 Gent,
Belgium.*

Keywords: Ti-base alloy, carburization, steam cracking, pretreatment, cracking, thermal cracking, oxidation, ethane, coke formation, aging, jet stirred reactor, cyclic aging

* Corresponding author: Technologiepark 914, 9052 Gent, Belgium;
Kevin.VanGeem@Ugent.be

Introduction

One of the dominant processes to manufacture light olefins is steam cracking of hydrocarbons. The major problem occurring during this process is the coke deposition on the inner wall of the tubular crackers. The formed coke layer reduces the available reactant cross-sectional area causing elevated pressure drop along the reactor. These promote bimolecular over monomolecular reactions, decreasing the olefin selectivity. As a result, more energy is required to maintain the cracking severity and the desired selectivity^{1, 2}. At a certain point, either when the metallurgic limits are reached or the pressure drop over the reactor is excessive, the operation is ceased and decoking of the reactor is necessary; typically for 48 h. The latter affects negatively the process finance³. In an effort to mitigate coke formation several anti-coking technologies have been evolved, namely 3-D reactor technologies⁴⁻⁶, application of additives⁷⁻¹⁰ and use of advanced surface technologies¹¹⁻¹⁷.

The present work, testing the cracking behavior of a Ti-base alloy, belongs clearly in the last technologies category. Titanium is used most of the times to enrich the composition of a high temperature alloy in concentrations of 0 to 10 wt %¹⁸ aiming at an increased rigidity. However, to the best of the knowledge of the authors, it has not been used as base material for crackers, therefore no quantitative coking behavior observations are available. In order to evaluate the coking performance of this alloy under ethane steam cracking conditions, an experimental study was performed in a jet-stirred reactor thermogravimetric set-up. As a first step, the optimum pretreatment of Fe-Ni-Cr alloys was applied and compared with a pretreatment increased by 100 K temperature. This, based on the available literature¹⁹⁻²², aimed at a better oxidation of the surface, thus at an improved coking behavior of the material (see Figure 1). According to that a factor 8 increase in the absolute weight of oxides is expected by increasing the temperature from 1173 K to 1273 K.

The target was partially achieved, the results proved decreased coking rates of the Ti-base alloy after the new treatment in comparison with the standard treatment used for Fe-Ni-Cr alloys, at the expense of the pronounced formation of Carbon oxides. However, the coking performance was still not better than the industrially representative alloy, while the tested Ti-base alloy coupons were partially or fully broken in pieces or slices after application of cyclic aging and cooling down back to ambient conditions. Therefore, the tested Ti-base alloy was not characterized as industrially interesting.

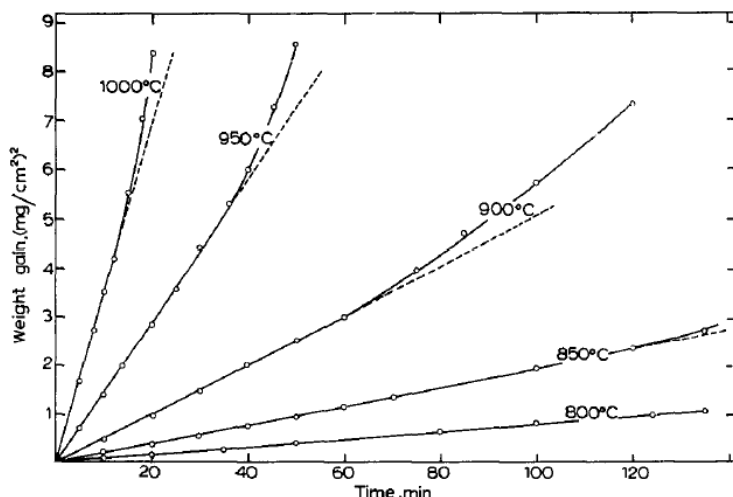


Figure 1. Effect of temperature on the oxides gain over time

Experimental Set-up

A picture of the jet-stirred reactor (JSR) is illustrated in Figure 2. The reactor is entirely made of quartz, including the nozzles and walls, minimizing coke formation on the inner surface. A small flat coupon is placed in the JSR, suspended from the arm of an electro-balance. Typically, the samples are cut by electro-erosion from the internal surface of industrial tubes to dimensions 10 mm x 8 mm x 1 mm. The coupons are polished before assembly to a Ra roughness of 2.6 μm .

The electro-balance can measure the weight difference of the coupons on-line with an accuracy of $1 \mu\text{g s}^{-1}$, giving the advantage of actual coking rate values over time. The reactor effluent is quenched to prevent further cracking and coking and its composition is measured online with the aid of two gas chromatographs (GC). Nitrogen is used as internal standard, while the detection limit ranges from methane to naphthalene, satisfactory for Ethane cracking²³.

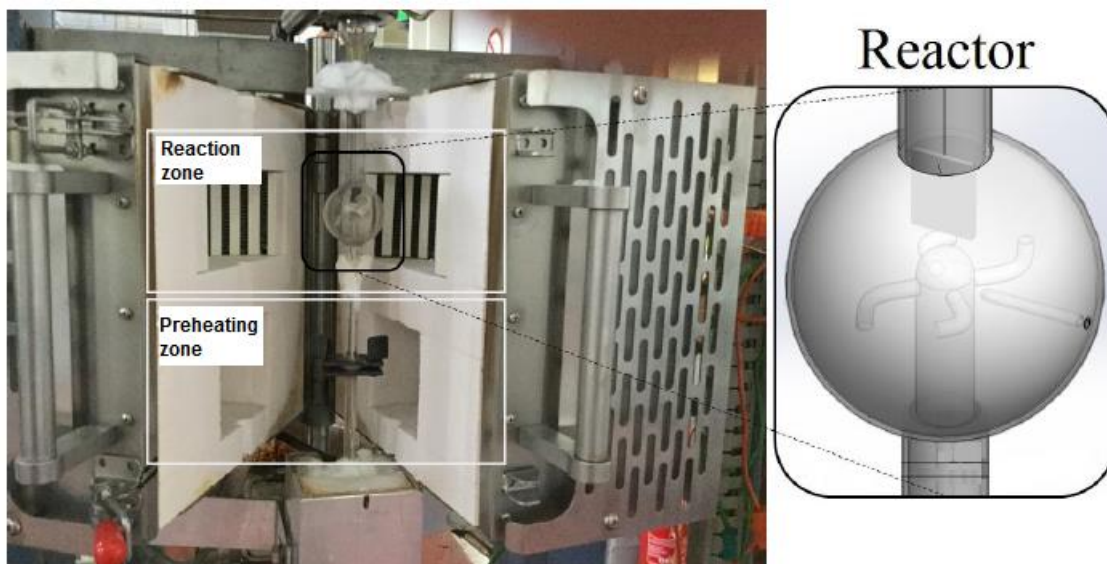


Figure 2. Jet stirred reactor used for coking behavior evaluation during steam cracking

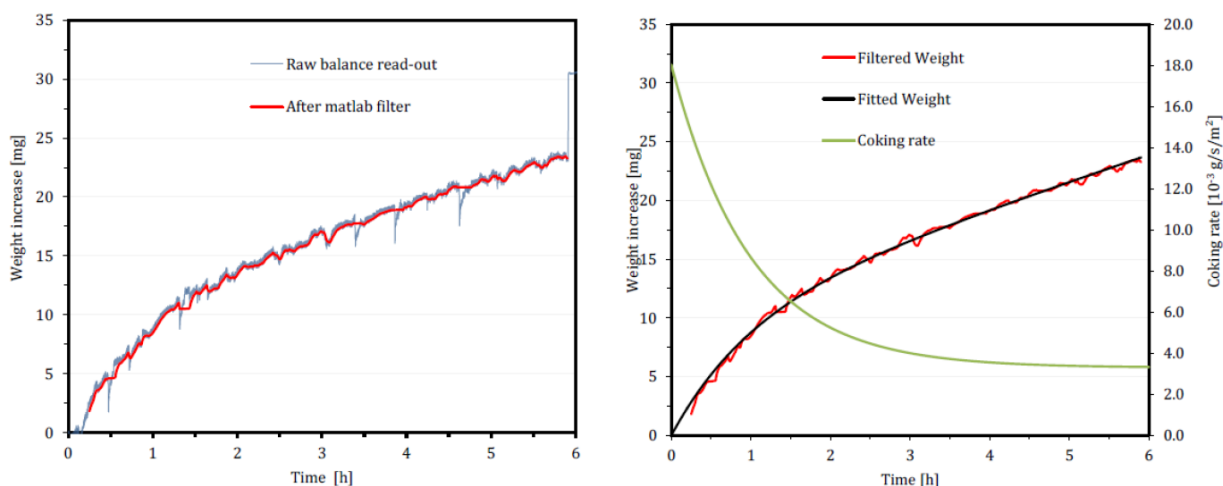


Figure 3. JSR data processing.

A graphical visualization of the data processing as executed by the MATLAB program is shown in Figure 3. In this work, the mean measured value between the initial 15 and 60 minutes is determined as initial coking rate characterizing the catalytic coking mechanism. The asymptotic or pyrolytic coking rate is related to the radical coking mechanism and is reported as the mean measured coking rate between the 5th and 6th hour of cracking.

The samples extracted after the experiment, are ex-situ analyzed by means of SEM and EDX. Similarly to Figure 4, surface and cross sectional analyses are performed aiming at a better understanding of the phenomena occurring during and before cracking.

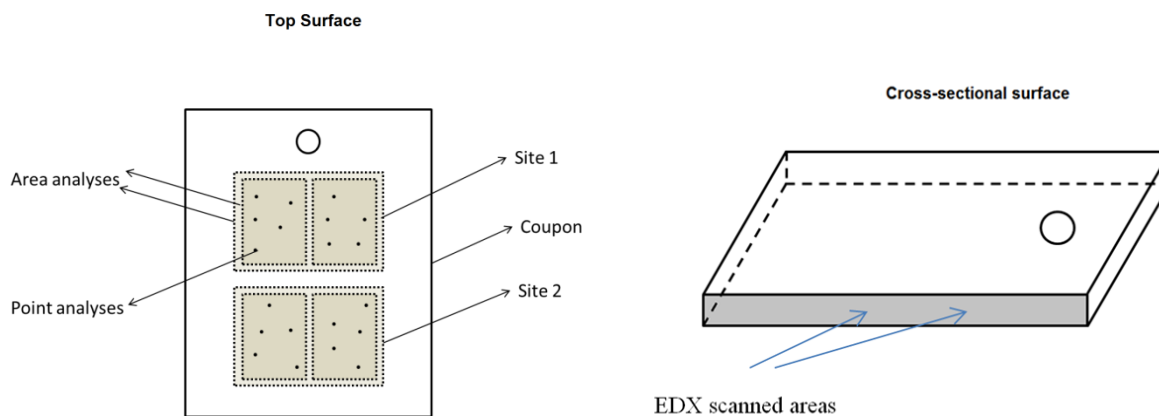


Figure 4. SEM and EDX analysis performed for the JSR samples

Experimental Results

The coking performance of the new Ti-base alloy under ethane steam cracking conditions was evaluated in the JSR set-up of LCT. Initially, the effect of the in-situ pretreatment was evaluated under blank ethane steam cracking conditions.

As mentioned above, a higher temperature pre-oxidation - 1273 K instead of 1173 K - than the typically applied for Fe-Ni-Cr alloys can increase significantly the absolute weight of oxides formed on Titanium^{20, 21}. Based on previous work the formation of a uniform and thick oxide layer can improve the anti-coking behavior of a material^{11, 12}. However, to the

best of the knowledge of the authors, no coking rates results are available for Ti-base alloys.

Table 1 and

Table 2 summarize the experimental conditions and sequences under the two different pretreatments.

Table 1. Conditions of the two different applied pretreatments

Pretreatment	Id	Steps		
		1	2	3
Standard pretreatment	A	$6.7 \cdot 10^{-3}$ NI s ⁻¹ of Air; 14h; T=1023 K	1:1 8.15 · 10 ⁻³ NI s ⁻¹ of Air:N ₂ ; 30 min; T=from 1023 K to 1173 K	$8.15 \cdot 10^{-3}$ NI s ⁻¹ of Air and $6.67 \cdot 10^{-6}$ kg s ⁻¹ Steam; 15min ; T=1173 K
High Temperature Preoxidation + Steam Treatment at higher temperature	B	$6.7 \cdot 10^{-3}$ NI s ⁻¹ of Air; 14h; T=1273 K	1:1 8.15 · 10 ⁻³ NI s ⁻¹ of Air:N ₂ ; 30 min; T=from 1023 K to 1273 K	$8.15 \cdot 10^{-3}$ NI s ⁻¹ of Air and $6.67 \cdot 10^{-6}$ kg s ⁻¹ Steam; 15min ; T=1273 K

Table 2. Experimental sequence during the two performed pretreatments.

A	1023 K Air	1023->1173 K N ₂ +Air	1173 K Air+H ₂ O	1173 K C ₂ H ₆ +H ₂ O	1023->1173 K N ₂ +Air	1173 K Air+H ₂ O	1173 K C ₂ H ₆ +H ₂ O	1023->1173 K N ₂ +Air	1173 K Air+H ₂ O	1173->273 K He	
	In situ Pre-oxidation 14 h	mild Pre-oxidation 30 min	Steam Treatment 15 min	1st coking cycle of 6 h	Decoking 30min	Steam Treatment 15 min	2nd-8th coking cycle of [2nd, 3rd and 8th of 6 h, 4-7th of 1 h]	Decoking 30 min	Steam Treatment 15 min	cooling down	time
B	1273 K Air	1023->1273 K N ₂ +Air	1273 K Air+H ₂ O	1173 °C C ₂ H ₆ +H ₂ O	1023->1273 K N ₂ +Air	1273 K Air+H ₂ O	1173 K C ₂ H ₆ +H ₂ O	1023->1273 K N ₂ +Air	1273 K Air+H ₂ O	1273->273 K He	
	In situ Pre-oxidation 14 h	High T Pre-oxidation 30 min	Steam Treatment 15 min	1st coking cycle of 6 h	Decoking at higher T 30 min	Steam Treatment 15 min	2nd-8th coking cycle of [2nd, 3rd and 8th of 6 h, 4-7th of 1 h]	Decoking at higher T 30 min	Steam Treatment 15 min	cooling down	time

Table 3 illustrates the most important mass yields during ethane cracking. For a better comparison the effluent results of a typically used material are also included in the presented yields. A factor 10 and 300 increased values of CO, for the typical and higher temperature pretreatment respectively, were measured over the 8 cracking cycles in

comparison with the Fe-Ni-Cr alloy. For CO₂, the effect was less pronounced; only after application of the high temperature pre-oxidation (b) an increase of a factor 3 was observed. In addition, the increase of Carbon oxides is followed by an increase of H₂. A minor decrease of CH₄ is also noticed, however it is still within the error margin of measured values. The observations support the idea that Ti and/or Ti-oxides present on the surface have a catalytic effect towards coke gasification. These results already prove that the Ti-base alloy is significantly worse than the reference material.

Table 3. Averaged (over the 8 cracking cycles) mass product yields. Ethane steam cracking: $F_{HC} = 29.18 \times 10^{-6} \text{ kg s}^{-1}$, $\delta = 0.33 \text{ kg}_{H_2O} \text{ kg}^{-1}_{HC}$, $T_{reactor} = 1173.15 \text{ K}$, $P = 101.35 \text{ kPa}$, $F_{H_2O} = 9.72 \times 10^{-6} \text{ kg s}^{-1}$.

Components [wt%]	Fe-Ni-Cr alloy A	Ti-base alloy A	Ti-base alloy B
H ₂ [± 0.07]	4.24	4.39	4.45
CO ₂ [± 0.003]	0.006	0.005	0.019
CO	0.05 ¹	0.56 ²	1.87 ³
CH ₄ [± 0.21]	6.99	6.97	6.91
C ₂ H ₆ [± 0.52]	30.13	30.19	30.06
C ₂ H ₄ [± 0.25]	49.86	49.61	49.57
C ₃ H ₈ [± 0.03]	0.11	0.11	0.11
C ₃ H ₆ [± 0.02]	0.74	0.70	0.69
C ₂ H ₂ [± 0.05]	1.38	1.46	1.41
1,3-C ₄ H ₆ [± 0.07]	2.00	1.93	1.89
Benzene [± 0.13]	2.46	2.53	2.53

¹ [± 0.008], ² [± 0.07], ³ [± 0.35]

Nevertheless, coking rates results are also processed and summarized in Table 4. For a qualitative comparison the results of reference material during continuous addition of DMDS are presented as well. Depending on the cracking cycle the Ti-base alloy performs significantly worse than the reference material. The increased temperature pretreatment improves the coking rates of the Ti-base alloy. However, this improved coking behavior still keeps the Ti-base alloy out of competition against the blank reference coking behavior. In terms of anti-coking performance, the Ti-base alloy is placed between the reference during steam cracking with continuous addition of DMDS and the reference with no DMDS.

Additionally, the reference material maintains a rather stable coking behavior over cyclic aging, while the sample of the Ti-base alloy shows increased coking after several cycles.

Table 4. Calculated initial (average 15min-60min) and asymptotic (average 5h-6h) coking rates. Ethane steam cracking: $F_{HC}= 29.18 \times 10^{-6} \text{ kg s}^{-1}$, $\delta= 0.33 \text{ kg}_{H_2O} \text{ kg}^{-1}_{HC}$, $T_{reactor}= 1173.15 \text{ K}$, $P= 101.35 \text{ kPa}$, $F_{H_2O}=9.72 \times 10^{-6} \text{ kg s}^{-1}$.

Alloy	Fe-Ni-Cr alloy	Ti-base alloy	Ti-base alloy	Fe-Ni-Cr alloy
Conditions	Blank	Blank	Blank	CA
Pretreatment	A	A	B	A
Cracking Temperature (K)	1173	1173	1173	1173
dilution	0.33	0.33	0.33	0.33
CA DMDS (ppmw S per HC)	0	0	0	41
Cc	Coke formed (mg)			
1	1.29	5.48	3.66	7.55
2	1.26	9.01	4.99	8.38
3	1.41	7.43	4.82	8.66
4	0.60	3.57	2.93	4.12
5	0.67	3.03	2.17	4.55
6	0.69	2.97	2.13	4.53
7	0.47	2.95	2.32	4.51
8	1.19	7.69	5.35	12.46
Cc	Initial coking rate [10^{-6} kg/s/m^2]			
1	0.71	1.73	1.23	3.03
2	0.67	3.26	1.81	4.74
3	0.86	3.65	2.59	4.23
4	0.85	3.80	3.11	5.85
5	0.96	3.91	2.76	6.45
6	0.97	3.80	2.70	6.42
7	0.67	3.79	2.79	6.39
8	0.63	3.27	2.46	5.29
Cc	Asymptotic coking rate [10^{-6} kg/s/m^2]			
1	0.22	1.06	0.61	1.53
2	0.22	1.58	0.83	1.43
3	0.23	0.93	0.53	1.61
8	0.21	1.25	0.74	2.47

The most discouraging result obtained by the Ti-base Alloy coupons was their behavior after cooling down to ambient conditions. Most specifically, the coupons broke either in slices or in smaller pieces. In Figure 5, an indication of the thickness decrease after cracking and of the thickness of the slices is given. Clearly, thick oxides are formed during oxidation of Ti, making the coupon more brittle as material towards mechanical stresses. The latter leads to the formation of cracks due to the mechanical stresses evolved during cooling down. An additional example of a cracked coupon is given in Figure 6. For a better understanding of this phenomenon SEM and EDX analysis are performed.

The cross sectional analyses of the two samples treated at the two different temperatures reveal part of the phenomenon occurring in this study (Figure 7). In the standard temperature, 1173 K, 0.1 to 0.2 μm thick oxides are formed and spalling off the

coupon from both sides leaving no oxide covering the surface. At 1273 K, thick oxides are formed leading to oxidation of almost the whole coupon volume. Clearly the oxides that are formed are quite brittle. Thus, they are separating from the core of the coupon. In the case of the increased temperature oxidation, the core is too thin, therefore the crack is propagating causing breakage of the coupon in smaller pieces.

Combining the above experimental results with the formation of cracks on the samples' surface can give a fruitful insight on the phenomenon. Based on the increased values of carbon oxides and H_2 differences of the yields, an increased catalytic surface of the Ti-base alloy samples can be assumed. That most probably derived from the presence of the surface cracks. As a result both coke formation and coke gasification were catalyzed.



Figure 5. Thickness values of the Ti-base alloy before cracking (left), after cracking (middle) and of a broken slice (right), pretreated at 1173 K.



Figure 6. Broken Ti-base alloy coupon after cracking pretreated at 1273 K.

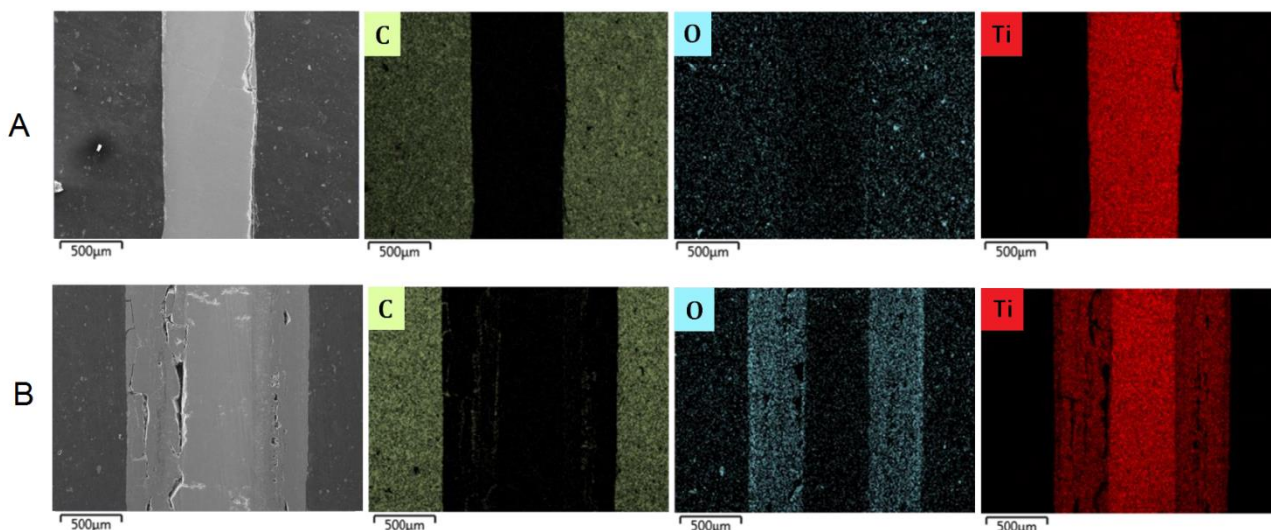


Figure 7. SEM and EDX cross sectional analysis of the two pretreatments. A is referring to temperature of 1173 K and B to 1273 K.

Conclusions

A newly tested Ti-base alloy was evaluated under industrially relevant ethane steam cracking conditions. Outrageously increased values of CO, both for the standard and higher temperature pretreatment, were measured over the 8 cracking cycles in comparison with a typical Fe-Ni-Cr alloy under the same experimental conditions. Notable increase of the CO₂ was observed between the higher temperature pre-oxidation (b) and the typical pre-oxidation used for Fe-Ni-Cr (a) when applied to the Ti-base alloy. No significant difference was observed for the CO₂ values of Ti-base alloy in comparison with the reference material in the standard treatment.

The increase of Carbon oxides is followed by a slight increase of H₂, supporting the idea that Ti and Ti-oxides are catalytic towards coke gasification. The significant differences in terms of gas phase composition can be explained by the increased available surface interacting with the gas phase. Clearly at the points of crack formation coke formation and gasification was catalyzed, affecting the gas phase product distribution.

Additional surface analysis will lead to a better understanding of the crack formation phenomenon observed in these alloys. Judging by these experimental results, the use of the Ti-base alloy in an industrial cracker is considered highly risky and certainly not beneficial in terms of coking or carbon oxides formation.

References

1. Rao, M. R.; Plehiers, P. M.; Froment, G. F., The coupled simulation of heat transfer and reaction in a pyrolysis furnace. *Chemical engineering science* **1988**, 43, (6), 1223-1229.
2. Stefanidis, G.; Merci, B.; Heynderickx, G. J.; Marin, G. B., CFD simulations of steam cracking furnaces using detailed combustion mechanisms. *Computers & chemical engineering* **2006**, 30, (4), 635-649.
3. Heynderickx, G.; Schools, E.; Marin, G., Optimization of the decoking procedure of an ethane cracker with a steam/air mixture. *Industrial & engineering chemistry research* **2006**, 45, (22), 7520-7529.
4. Brown, D. J., Internally finned radiant coils: A valuable tool for improving ethylene plant economics. In *6th EMEA Petrochemicals Technology Conference*, London, UK, 2004.
5. Albano, J.; Sundaram, K.; Maddock, M. *Application of extended surfaces in pyrolysis coils*; New York, NY; American Institute of Chemical Engineers: 1988.

6. Schietekat, C. M.; van Goethem, M. W. M.; Van Geem, K. M.; Marin, G. B., Swirl flow tube reactor technology: An experimental and computational fluid dynamics study. *Chemical Engineering Journal* **2014**, 238, (0), 56-65.
7. Reyniers, M.-F. S. G.; Froment, G. F., Influence of Metal Surface and Sulfur Addition on Coke Deposition in the Thermal Cracking of Hydrocarbons. *Industrial & Engineering Chemistry Research* **1995**, 34, (3), 773-785.
8. Wang, J.; Reyniers, M.-F.; Marin, G. B., Influence of Dimethyl Disulfide on Coke Formation during Steam Cracking of Hydrocarbons. *Industrial & Engineering Chemistry Research* **2007**, 46, (12), 4134-4148.
9. Wang, J.; Reyniers, M.-F.; Marin, G. B., The influence of phosphorus containing compounds on steam cracking of n-hexane. *Journal of Analytical and Applied Pyrolysis* **2006**, 77, (2), 133-148.
10. Wang, J.; Reyniers, M.-F.; Van Geem, K. M.; Marin, G. B., Influence of Silicon and Silicon/Sulfur-Containing Additives on Coke Formation during Steam Cracking of Hydrocarbons. *Industrial & Engineering Chemistry Research* **2008**, 47, (5), 1468-1482.
11. Muñoz Gandarillas, A. E.; Van Geem, K. M.; Reyniers, M.-F.; Marin, G. B., Influence of the Reactor Material Composition on Coke Formation during Ethane Steam Cracking. *Industrial & Engineering Chemistry Research* **2014**, 53, (15), 6358-6371.
12. Muñoz Gandarillas, A. E.; Van Geem, K. M.; Reyniers, M.-F.; Marin, G. B., Coking Resistance of Specialized Coil Materials during Steam Cracking of Sulfur-Free Naphtha. *Industrial & Engineering Chemistry Research* **2014**, 53, (35), 13644-13655.
13. Verdier, G.; Carpentier, F., Consider new materials for ethylene furnace applications: An innovative metallurgy solves maintenance issues. *Hydrocarbon processing* **2011**, 90, (5), 61-62.
14. Wolpert, P.; Ganser, B.; Jakobi, D.; Kirchheiner, R., Using steam; tube with uniform cross-section; pyrolysis; antideposit agents; interior fins; swirling gas flow. In Google Patents: 2005.
15. Jakobi, D.; van Moesdijk, C.; Karduck, P.; von Richthofen, A., Tailor-made materials for high temperature applications: New strategies for radiant coil material development. *CORROSION 2009* **2009**.
16. Jakobi, D.; Karduck, P.; von Richthofen, A. F., The High-Temperature Corrosion Resistance of Spun-Cast Materials for Steam-Cracker Furnaces-A Comparative Study of Alumina-and Chromia-Forming Alloys. *CORROSION 2013* **2013**.
17. Asteman, H.; Hartnagel, W.; Jakobi, D., The Influence of Al Content on the High Temperature Oxidation Properties of State-of-the-Art Cast Ni-base Alloys. *Oxidation of Metals* **2013**, 80, (1-2), 3-12.
18. Petrone, S. S. A.; Mandyam, R. C.; Wysiekierski, A. G., Surface alloyed high temperature alloys. In Google Patents: 2000.
19. Kumar, S.; Sankara Narayanan, T. S. N.; Ganesh Sundara Raman, S.; Seshadri, S. K., Thermal oxidation of Ti6Al4V alloy: Microstructural and electrochemical characterization. *Materials Chemistry and Physics* **2010**, 119, (1-2), 337-346.
20. Kofstad, P.; Anderson, P. B.; Krudtaa, O. J., Oxidation of titanium in the temperature range 800–1200°C. *Journal of the Less Common Metals* **1961**, 3, (2), 89-97.
21. Kofstad, P., High-temperature oxidation of titanium. *Journal of the Less Common Metals* **1967**, 12, (6), 449-464.
22. Kumar, S.; Narayanan, T. S. N. S.; Raman, S. G. S.; Seshadri, S. K., Thermal oxidation of CP-Ti: Evaluation of characteristics and corrosion resistance as a function of treatment time. *Materials Science and Engineering: C* **2009**, 29, (6), 1942-1949.
23. van Goethem, M. W. M.; Barendregt, S.; Grievink, J.; Verheijen, P. J. T.; Dente, M.; Ranzi, E., A kinetic modelling study of ethane cracking for optimal ethylene yield. *Chemical Engineering Research and Design* **2013**, 91, (6), 1106-1110.